BIOCHEMISTRY
including biophysical chemistry & molecular biology
Article

Biochemistry **2009,** *48,* 11449–11457 11449
DOI: 10.1021/bi901479b

Characterization of a Ras Mutant with Identical GDP- and GTP-Bound Structures[†,‡]

Bradley Ford,[§] Sean Boykevisch,[∥] Chen Zhao,[∥] Simone Kunzelmann,[⊥] Dafna Bar-Sagi,[∥] Christian Herrmann,[⊥] and Nicolas Nassar*[,§]

[§]*Department of Physiology and Biophysics, Stony Brook University, Stony Brook, New York 11794-8661,* [∥]*Department of Molecular Genetics and Microbiology, Stony Brook University, Stony Brook, New York 11794-5222, and* [⊥]*Ruhr-Universität Bochum, Physikalische Chemie I, Fakultät für Chemie, Universitätsstrasse 150, 44780 Bochum, Germany*

Received August 24, 2009; Revised Manuscript Received October 29, 2009

ABSTRACT: We previously characterized the G60A mutant of Ras and showed that the switch regions of the GTP-bound but not the GDP-bound form of this mutant adopt an "open conformation" similar to that seen in nucleotide-free Ras. Here, we mutate Lys147 of the conserved ^{145}SAK^{147} motif in the G60A background and characterize the resulting double mutant (DM). We show that RasDM is the first structure of a Ras protein with identical GDP- and GTP-bound structures. Both structures adopt the open conformation of the active form of RasG60A. The increase in the accessible surface area of the nucleotide is consistent with a 4-fold increase in its dissociation rate. Stopped-flow experiments show no major difference in the two-step kinetics of association of GDP or GTP with the wild type, G60A, or RasDM. Addition of Sos fails to accelerate nucleotide exchange. Overexpression of the G60A or double mutant of Ras in COS-1 cells fails to activate Erk and shows a strong dominant negative effect. Our data suggest that flexibility at position 60 is required for proper Sos-catalyzed nucleotide exchange and that structural information is somehow shared among the switch regions and the different nucleotide binding motifs.

The conversion of Ras from a resting GDP-bound to an active GTP-bound protein is a key step in transmitting the activation of membrane-bound receptor tyrosine kinases to the initiation of gene transcription in the nucleus (*1*, *2*). The activation of Ras is a slow reaction that is accelerated in cells by guanine nucleotide exchange factors (GEFs),[1] members of the Cdc25 homology family of proteins including Sos. This conversion step has been the focus of extensive in vivo and in vitro studies because of its importance in initiating a variety of signaling cascades and its potential for being targeted in therapeutic intervention (*3*−*6*). By analogy to those of other G-proteins (*7*−*12*), the accepted scheme for Ras nucleotide exchange is that the tight binary Ras·GXP complex (GXP being GDP or GTP) dissociates into nucleotide-free Ras (hereafter NF-Ras) and free GXP. Subsequently, a GXP molecule binds to NF-Ras, and a new cycle of exchange can take place. The catalyzed nucleotide dissociation from Ras by a GEF was shown to follow the same reaction scheme described for Ras intrinsic nucleotide exchange with the formation of a Ras·GXP−GEF ternary complex that separates into a NF-Ras−GEF binary complex and free GXP (*13*). This reaction is further accelerated by a feedback mechanism through the binding of an activated Ras molecule to an allosteric site on Sos (*14*).

From a structural standpoint, the activation of Ras can be explained by its cycling between the "closed" and "open" conformations. These refer to the conformation of the switch regions of Ras as seen in the presence and absence of the nucleotide, respectively. In the closed conformation (*15*, *16*), the switch regions close on the nucleotide-binding site to stabilize the GXP, while they move away from the nucleotide to facilitate its dissociation in the open conformation (*17*). One accepted role for Ras specific GEFs is their ability to stabilize NF-Ras.

We previously characterized the Ala for Gly mutant of Ras at position 60, RasG60A. We showed that whereas the mutation does not affect the intrinsic rate of GDP or GTP dissociation, the binding of Sos to RasG60A fails to accelerate nucleotide dissociation. Instead, the presence of Sos results in a stable RasG60A·GTP−Sos and to a lesser extent a RasG60A·GDP−Sos ternary complex (*18*). From a structural point of view, the switch regions of the active but not the inactive form of this mutant adopt the open conformation reminiscent of NF-Ras (*17*). Phe28 does not stabilize the guanine base, as is the case in all nucleotide-bound structures of Ras. Rather, its phenyl group is displaced ∼15 Å from the guanine base and is replaced with the long aliphatic side chain of Lys147 such that the guanine base is sandwiched between the lysine side chains of the conserved ^{116}NKXD^{119} and ^{145}SAK^{147} motifs.

To explain the inability of Sos to stimulate dissociation of the nucleotide from RasG60A, we argued that the absence of a flexible glycine at position 60 is one likely reason. Alternatively, Sos is unable to destabilize the Lys147−guanine interaction (*18*). To shed light on the role of Lys147 in nucleotide exchange, we mutated Lys147 to Ala in the G60A background. Here, we

[†]Research in N.N.'s laboratory is supported in part by grants from the National Institutes of Health (CA-115611), the National Science Foundation (MCB-0316600), and the U.S. Department of Defense (NF060060). The National Synchrotron Light Source is supported by the Department of Energy and NIH, and beamline X26C is supported in part by Stony Brook University and its Research Foundation. B.F. was supported by a Medical Training Grant.

[‡]The coordinates of the GDP- and GppCH$_2$p-bound forms of RasDM were deposited in the Protein Data Bank as entries 2GCK and 2GCM, respectively.

*To whom correspondence should be addressed: Department of Physiology and Biophysics, Basic Sciences Tower, Stony Brook University, Stony Brook, NY 11794-8661. Telephone: (631) 444-3521. Fax: (631) 444-3432. E-mail: nicolas.nassar@sunysb.edu.

[1]Abbreviations: GEF, guanine nucleotide exchange factor; GXP, GDP or GTP; Ni-NTA, nickel-nitrilotriacetic acid; HPLC, high-performance liquid chromatography; DTT, dithiothreitol; WT, wild-type; NF, nucleotide-free; DM, double mutant; mant, *N*-methylanthraniloyl; RafRBD, Ras binding domain of Raf kinase; PDB, Protein Data Bank.

Published on Web 11/02/2009

Table 1: Data Collection and Refinement Statistics

	RasG60A/K147A		RasK147A
	GDP	$GppCH_2p$	GDP
resolution range (Å)	28.0−1.35	50.0−1.80	50.0−1.50
R_{sym},[a] % overall (last shell)	6.0 (58.6)	8.0 (50.4)	10 (53.1)
completeness, % overall (last shell)	98.4 (96.8)	99.2 (99.4)	99.9 (99.9)
multiplicity, overall (last shell)	8.8 (8.4)	6.6 (6.3)	10.8 (9.5)
no. of unique reflections	37822	16122	31903
no. of water molecules	191	148	237
overall *B* factor (Å^2)	15.0	20.7	17.8
R_{free},[b] % overall (last resolution shell)	17.6 (25.8)	21.8 (32.2)	19.2 (25.1)
R_{cryst},[c] % overall (last resolution shell)	16.1 (18.6)	18.0 (23.6)	17.6 (22.1)
root-mean-square deviation in bond lengths (Å)	0.013	0.014	0.011
root-mean-square deviation in bond angles (deg)	1.541	1.381	1.345
estimated coordinate error[d] (Å)	0.051/0.026	0.135/0.076	0.064/0.038
Ramachandran plane[e] (%)	94.7/5.3	94.7/5.3	94/6.0

[a] $R_{sym} = \sum_{i,hkl}|\langle I(hkl)\rangle - I_i(hkl)|/\sum_{i,hkl}I_i(hkl)$. The last resolution shells are 1.38−1.35 and 1.84−1.80 Å for the GDP- and $GppCH_2p$-bound forms of RasDM, respectively, and 1.53−1.50 Å for RasK147A. [b] $R_{free} = \sum_{(hkl)\varepsilon T}||F_{obs}| - |F_{calc}||/\sum_{(hkl)\varepsilon T}|F_{obs}|$, where T is the test set (*41*) obtained by randomly selecting 5% of the data. [c] $R_{cryst} = \sum_{(hkl)}||F_{obs}| - |F_{calc}||/\sum_{(hkl)}|F_{obs}|$. [d] Estimated coordinate error based on R_{free}/maximum likelihood. [e] Most favored/additional allowed regions.

present the structural and biochemical characterization of the RasG60A/K147A double mutant, hereafter RasDM.

EXPERIMENTAL PROCEDURES

Crystallization and Structure Determination. Wild-type Ras (hereafter WT-Ras), RasG60A, RasK147A, and RasDM- (residues 1−166) were cloned as His-tagged proteins in the pProEX-HTb vector and expressed in *Escherichia coli* strain BL21(DE3) as described in ref *19*. Proteins were purified on a Ni-NTA column (Qiagen) followed by a gel filtration column (Superdex 200, GE Healthcare). The GDP-bound nucleotide was exchanged with the slowly hydrolyzable GTP analogue $GppCH_2p$ (*20*), and exchange was confirmed on a HPLC C18 reverse phase column. For X-ray diffraction experiments, crystals were grown at 20 °C by mixing 4 μL of RasDM at 20 mg/mL in 20 mM HEPES, 150 mM NaCl, and 10 mM $MgCl_2$ (pH 7.5) and 4 μL of the reservoir. For the GDP-bound form, the reservoir consisted of 30% (w/v) PEG2000 monomethyl ether, 0.2 M magnesium sulfate, and 0.1 M Tris-HCl (pH 8.0). For the $GppCH_2p$-bound form, the reservoir consisted of 25% (w/v) PEG5000 monomethyl ether, 0.15 M magnesium acetate, 0.1 M HEPES (pH 7.0), and 0.3% hydrogen peroxide. The GDP- and $GppCH_2p$-bound forms crystallized in space group *I*222 (a = 34.3 Å, b = 83.0 Å, and c = 120.5 Å) with one copy in the asymmetric unit. For the RasK147A mutant, the reservoir consisted of 22% PEG8000, 50 mM magnesium acetate, and 0.1 M Tris-HCl (pH 7.5). The K147A mutant crystallized in space group *R*32 (a = 92.9 Å and c = 118.7 Å). In each case, data were collected on beamline X26C at the National Synchrotron Laboratory Source (NSLS), Brookhaven, on a 2K × 2K CCD detector (ADSC) and processed with the HKL2000 package (*21*). The structures of RasDM were determined by molecular replacement (*22*) using the deposited coordinates of RasG60A·GppNHp as a search model [PDB entry 1XCM (*18*)]. The structures were refined using anisotropic temperature factors or TLS groups (*23*) in REFMAC (*24*) against 1.35 or 1.80 Å diffraction data, respectively. Stereochemistry was checked with PROCHECK (*25*). Data collection and refinement statistics are summarized in Table 1.

Stopped-flow experiments were performed in an SFM-400 apparatus with MOS-200 optics (Bio-Logic, Grenoble, France). NF-Ras was prepared according to the protocol described by John (*20*). Briefly, GDP-bound Ras proteins were incubated with alkaline phosphatase (Sigma) in the presence of a 1.5-fold molar excess of $GppCH_2p$ until all GDP was degraded. Snake venom phosphodiesterase (Sigma) was then added. Once degradation of the $GppCH_2p$ was complete as monitored by HPLC, the proteins were exchanged on PD-10 columns into a buffer containing 50 mM Tris-HCl (pH 7.4), 5 mM $MgCl_2$, 2 mM DTE, and 10% glycerol and kept at −80 °C until needed. We investigated the mant-nucleotide (2′,3′-*N*-methylanthraniloyl) binding to NF-Ras proteins by mixing small volumes (50 μL) in <1 ms and recording the increase in fluorescence. The fluorescence was excited at 366 nm and monitored through a 420 nm cutoff filter. The ratio of the nucleotide to protein concentrations was at least 10:1, providing pseudo-first-order binding kinetics. The experimental data were fitted to an exponential function of the form $F(t) = at + b + c\exp(-k_{obs}t)$, from which the k_{obs} value is extracted. The linear part of $F(t)$ accounts for the photobleaching of the fluorophore. Stopped-flow experiments were conducted at 10 °C in 50 mM Tris-HCl (pH 7.4), 5 mM $MgCl_2$, and 2 mM DTE. Each data point was repeated three times and averaged. Binding of 2′-deoxy-3′-mantGTP to RasDM was assessed and showed no difference from that of the 2′/3′-mantGTP mixture.

Rate of Nucleotide Exchange. Ras (1 μM) was incubated in 10 mM HEPES (pH 7.5), 150 mM NaCl, 2 mM β-mercaptoethanol, 2 mM EDTA, and 5 μM mant-nucleotide (Molecular Probes) in a quartz cuvette. The mixture was adjusted to 10 mM $MgCl_2$ for 5 min, and the decrease in fluorescence was then monitored following the addition of 0.5 mM unlabeled GTP. The total reaction volume was 120 μL; all reactions were conducted at 25 °C, and fluorescence was monitored at each step with an excitation wavelength of 355 nm and an emission wavelength of 438 nm (5 nm slit widths on a Perkin-Elmer LS-50B luminescence spectrometer). Data were fitted to a single exponential from which k_{-2} was deduced (*18*).

ITC experiments were conducted as described in ref *26*. Briefly, binding of RafRBD (residues 51−131 of Raf kinase) to GppNHp-bound RasG60A was assessed at 25 °C using a VP-ITC microcalorimeter (MicroCal, Inc.). All proteins were extensively dialyzed against buffer containing 10 mM HEPES

(pH 7.5), 150 mM NaCl, and 2 mM $MgCl_2$, centrifuged, and degassed under vacuum immediately before use. The sample concentration was determined by averaging three measurements using Bradford reagent (*27*). RafRBD (218 μM) was injected into the temperature-controlled sample cell, which contained Ras proteins at ~20 μM. The change in heat generation was monitored for 4 min until equilibrium was reached before the next 10 s injection was started. Background heat generated from dilution of RafRBD was measured in control experiments where RafRBD was injected into buffer alone and subtracted from the integrated pulses. The data were averaged over three ITC experiments. N was 1.01 ± 0.04 for all measurements.

RafRBD Pull-Down Assay. GST−RafRBD protein (100 nM) was incubated with Ras proteins at the concentrations shown in Figure 3B in 1 mL of a solution containing 10 mM HEPES (pH 7.5), 150 mM NaCl, and 2 mM β-mercaptoethanol for 20 min at room temperature with gentle agitation. Glutathione−agarose beads [50 μL of a 50% slurry (Sigma)] were added to each tube for an additional 20 min. Beads were pelleted and washed twice with 1 mL of buffer and then loaded on a 12% SDS−PAGE gel. Blots were probed with pan-Ras antibody (Santa Cruz FL-189, 1:2000) and HRP-labeled anti-rabbit antibody (Santa Cruz SC-2004, 1:400) for Ras and with anti-GST (Santa Cruz SC-138, 1:800) and HRP-labeled anti-mouse antibody (Southern Biotech 1010-05) for RafRBD. Blots were developed with ECL Plus reagent (Amersham Biosciences) and exposed on a Kodak 440CF Image Station.

Sos Pull-Down Assay. Assays were performed as with the RafRBD pull-down assays. GST−Sos protein (100 nM) was incubated with Ras at the concentrations shown in Figure 3A.

Cell Culture and Erk Activation Assay. COS-1 cells were maintained in Dulbecco's modified Eagle's medium (Invitrogen) supplemented with 10% fetal bovine serum. Cells were transfected with Fugene 6 (Roche) according to the manufacturer's instructions. Erk activation was assessed by cotransfecting Cos cells with HA-tagged Erk and the indicated T7-tagged Ras constructs. The cells were allowed to express for a total of 24 h prior to serum starvation for 8 h. The cells were washed twice with ice-cold PBS and lysed in 400 μL of ice-cold buffer containing 10 mM Tris (pH 7.6), 150 mM NaCl, 1 mM EDTA, 10% glycerol, 1% Triton X-100, 1 mM Na_3VO_4, 1 mM NaF, 1 mM phenylmethanesulfonyl fluoride, 10 μg/mL pepstatin, 10 μg/mL aprotinin, 10 μg/mL leupeptin, and 10 mM benzamidine. For experiments that required growth factor stimulation, cells were stimulated with DMEM supplemented with or without 100 ng/mL EGF (Invitrogen) for 10 min at 37 °C prior to lysis. The lysates were clarified at 14000*g* for 15 min and were then incubated with anti-HA (12CA5) for 1 h at 4 °C. The immune complexes were incubated with protein A−Sepharose beads (Sigma) for 45 min at 4 °C. Immune complexes were washed four times with ice-cold lysis buffer and were eluted with SDS sample buffer. Samples were run on SDS−polyacrylamide gels and were transferred to nitrocellulose membranes (Schleicher & Schuell). The membranes were incubated with either anti-T7 (Novagen, 1:10000) or anti-Erk2 (Upstate Biotechnology, 1:1000) and phospho-Erk1/2 (Cell Signaling, 1:1000) antibodies. Subsequently, membranes were incubated with IRDye 800-conjugated goat anti-rabbit (Rockland, 1:10000) and Alexa-Fluor 680 goat anti-mouse (Molecular Probes, 1:10000) antibodies and visualized using the Odyssey Infrared Imaging System (LiCor). Relative Erk phosphorylation was assessed using Odyssey software and normalized to the total level of Erk expression.

RESULTS

Crystallographic Work. We have determined the crystal structures of RasDM bound to the slowly hydrolyzable GTP analogue $GppCH_2p$ and to GDP. The final models are refined to 1.8 and 1.35 Å resolution, respectively, with low crystallographic residuals and excellent stereochemistry (Table 1). Lys147 is part of the conserved ^{145}SAK^{147} motif in Ras-like GTPases. This motif interacts with O6 of the guanine base and stabilizes the conserved Phe28 and Asp119 of the ^{116}NKXD^{119} motif (*15*, *16*). Specifically, the long aliphatic side chain of Lys147 stacks against Phe28, which in turn stabilizes the guanine base of the nucleotide by stacking interactions. Overall, the K147A mutation did not affect the local structure of the ^{145}SAK^{147} loop.

Structure of RasDM·GppCH$_2$p. The three-dimensional structures of RasDM·$GppCH_2p$ and RasG60A·GppNHp are similar. The root-mean-square deviation (rmsd) calculated after the superposition of all 166 Cα atoms is 0.3 Å. The switch regions in the double mutant adopt the open conformations seen in the RasG60A·GppNHp crystal structure (*18*), which are reminiscent of NF-Ras (*17*) and make similar crystal contacts. Phe28 is not stabilizing the guanine base; instead, it is ~15 Å from its position in WT-Ras. Thr35 is not coordinating the Mg^{2+} ion; instead, a water molecule completes the octahedral coordination of the metal ion (Figure 1A). The triphosphate guanine nucleotide and the Mg^{2+} ion make identical coordination with the protein as in RasG60A·GppNHp with one important difference. The removal of the side chain of Lys147 further exposes the guanine base in RasDM to solvent. Consequently, the accessible surface area (*28*) of the triphosphate guanine nucleotide has increased from 95 to 195 Å^2 (Figure 1B), making it significantly more solvent exposed.

Structures of RasDM·GDP and RasK147A·GDP. Whereas the G60A mutation did not affect the overall structure of Ras·GDP (*18*), adding the K147A mutation resulted in a dramatic conformational change in the switch regions. Switch 1 adopts the open conformation where Phe28 is displaced from the guanine base. Consequently, RasDM adopts the same structure in the active and inactive forms (Figure 1A). This observation is supported by the isomorphism between the two crystals and the low calculated rmsd (0.163 Å) between the two structures. The open conformation results in a notable increase in the GDP-accessible surface area between WT-Ras (92 Å^2) and RasDM [197 Å^2 (Figure 1B)].

To test the hypothesis that the K147A mutation is alone responsible for the open conformation of RasDM, we determined the crystal structure of RasK147A·GDP (Table 1). The switch regions of RasK147A adopt a wild-type closed conformation also seen in RasG60A·GDP with Phe28 stabilizing the guanine nucleotide. This result shows that the K147A mutation alone is not responsible for the open conformation of RasDM.

Combined, our structural data demonstrate that Ala substitution for Gly60 and Lys147, which are more than 22 Å apart, but not either substitution alone is sufficient to induce an open conformation of the switch regions regardless of the nature of the bound guanine nucleotide. The RasDM is thus the first Ras protein that adopts the same three-dimensional structure in the active and inactive forms. Alternatively, one can envision that the switch domains of RasDM adopt in solution several conformations so that either the crystal packing selected the open conformation or only the open conformation crystallized. However, this idea is inconsistent with solution ^{31}P NMR spectra collected for RasG60A showing either a single static conformation or several conformations in fast exchange.

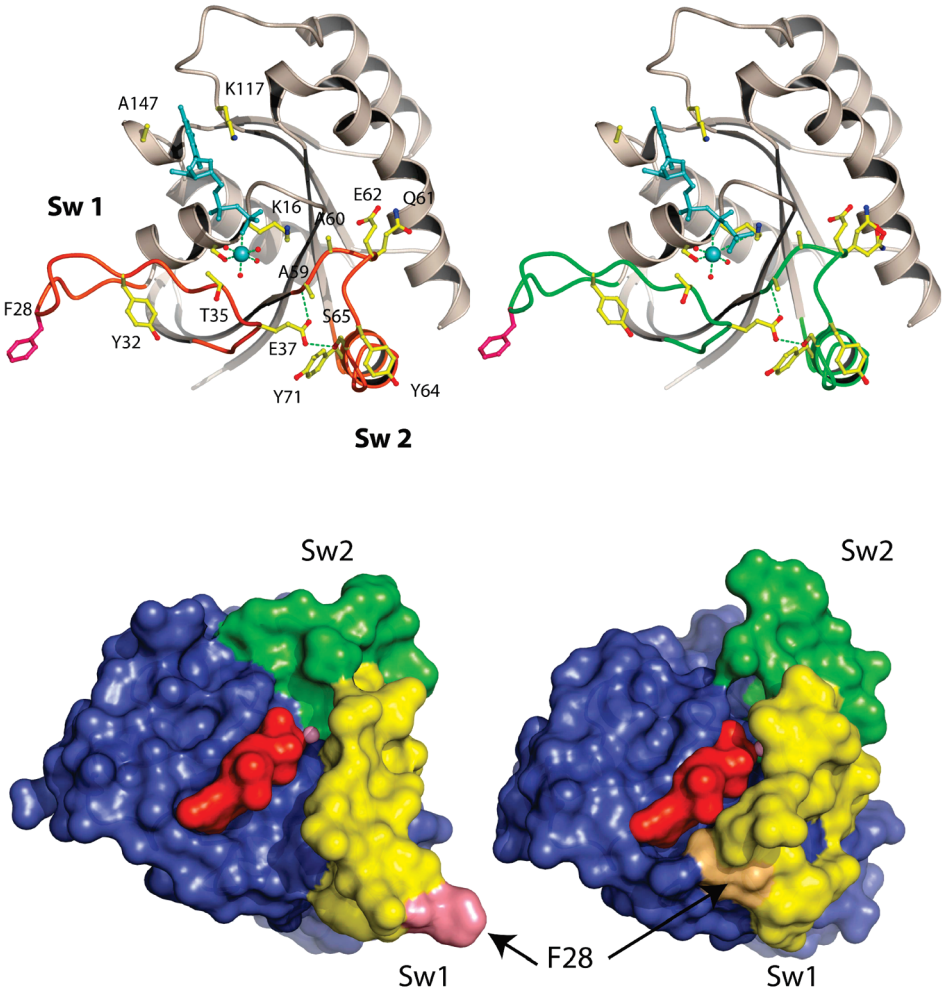

FIGURE 1: (A) Comparison of the GDP (left) and GppCH$_2$p (right) binding sites of RasDM. Ribbon representation of Ras (gray) with the switch regions (Sw 1 and Sw 2) colored orange or green. The nucleotides are shown in ball-and-stick format and the Mg^{2+} ion and its water coordinating molecules as cyan and red spheres. Dotted lines represent likely salt bridge and hydrogen bond interactions. For the sake of clarity, only important residues are shown. Figure generated with MOLSCRIPT (*40*) and Pymol (http://pymol.sourceforge.net/). (B) Comparison of GDP-bound RasDM (left) and WT-Ras (right) shown in surface representation. Switch 1 is colored yellow, switch 2 green, the nucleotide red, and the Mg^{2+} ion pink. Phe28 of switch 1 is highlighted for the sake of clarity.

Measurements of Guanine Nucleotide Binding Rate Constants. Since the G60A/K147A double mutation doubles the accessible surface area of the guanine nucleotides, we tested the hypothesis that the notable increase in solvent accessibility affects the properties of binding of the nucleotides to the open conformation of Ras. We prepared the nucleotide-free form of the Ras proteins according to the protocol described by John et al. (*20*) to measure the association kinetics of GDP and GTP in the presence of excess Mg^{2+}. We took advantage of the 2.5-fold increase in fluorescence upon association of the mant-nucleotides with Ras and used fast kinetics stopped-flow experiments to assess the binding of mant-GDP and mant-GTP, which were used as ligands. As shown in Figure 2, the apparent rate constants for the association reactions of the wild type, the G60A mutant, and RasDM do not show a linear dependence on the nucleotide concentration. This result demonstrates that the binding of GDP and GTP to the open conformation is a two-step reaction: a rapid step (step 1 in Scheme 1) followed by a slow isomerization reaction (step 2) as previously proposed for Ras (*20*). The equilibrium dissociation constant for the first step and the forward rate constant for the second step (K_1 and k_{+2}, respectively) derived from our fitting (see Experimental Procedures) as well as the resulting apparent association rate constant (k_{on}) are listed in Table 2. Overall, there is no significant change in the apparent association rate between the wild type and the Ras mutants. This result means that the second isomerization step, going from a loosely bound state to a tightly bound nucleotide, cannot be the closing of the switch regions on the guanine nucleotide-binding site going from the open to the closed conformation. If this were the case, we would have observed a one-step binding process characterized by a linear relationship of the observed rate constants as a function of the nucleotide concentration at least for the DM.

Next, we measured the intrinsic dissociation rate constants (k_{-2}) of the guanine nucleotides by taking advantage of the decrease in fluorescence of the mant group when mant-GDP or mant-GTP slowly dissociates from Ras in the presence of excess Mg^{2+}. The derived values of k_{-2} from our fluorescence experiments are listed in Table 2. Consistent with the increased nucleotide solvent accessibility seen in the three-dimensional structure, the intrinsic rates of dissociation of GDP (27×10^{-5} s^{-1}) and GTP (29×10^{-5} s^{-1}) from RasDM are ~4 times faster than for WT-Ras (6.5×10^{-5} and 8.1×10^{-5} s^{-1}, respectively) or RasG60A. This result suggests that the K147A mutation is responsible for the increase in the intrinsic rate of dissociation of the DM since the rates of the wild-type and G60A proteins are similar.

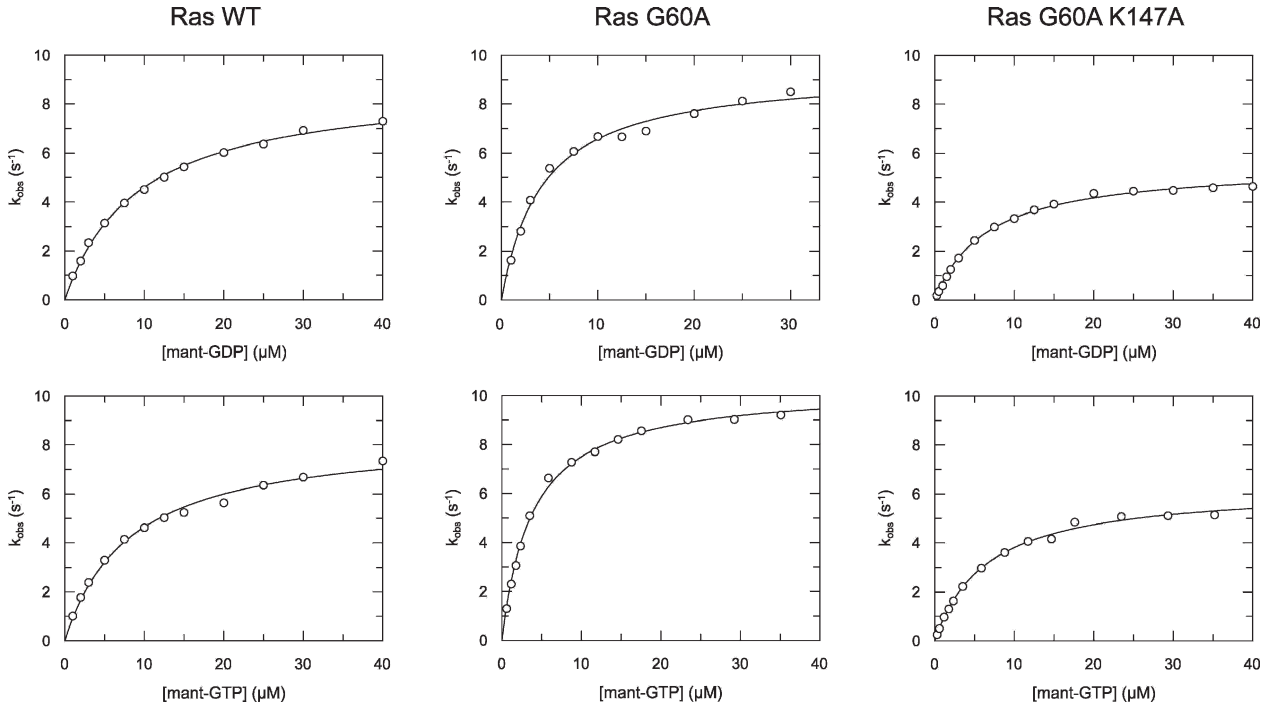

FIGURE 2: mant-GDP or mant-GTP binding to Ras proteins measured by fast kinetics stopped-flow experiments. In a stopped-flow apparatus, a 25 μM Ras solution was rapidly mixed with increasing concentrations of mant-GDP or mant-GTP, as indicated. The observed rate constants (k_{obs}) were obtained from the exponential fit of the fluorescence increase as described in Experimental Procedures, and the mean values were plotted against the mant-GDP and mant-GTP concentration. The data were fitted to a hyperbolic equation yielding K_1 and k_{+2}.

Scheme 1: Binding of Guanine Nucleotide GDP or GTP (shown as GXP) to Nucleotide-Free Ras in the Absence or Presence of an Exchange Factor Such as Sos[a]

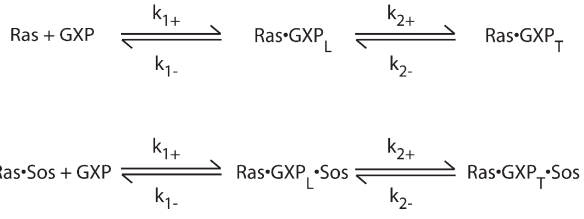

[a]The transition between the upper and lower reactions is achieved by the addition or removal of Sos. Adapted from ref *13*.

Measurement of k_{-2} and k_{on} allows us to calculate the dissociation constant K_d of GDP and GTP for the Ras mutants (Table 2). The double mutation has decreased the affinity of GDP (K_d = 319 pM) and GTP (K_d = 299 pM) for Ras by factors of 4.7 and 3.8, respectively, when compared to WT-Ras. This decrease is in line with the RasDM structure, but the decrease in nucleotide affinity does not correlate with the open conformation of Ras since the affinity of GTP (K_d = 36.1 pM) for RasG60A has increased by a factor of 2 when compared to the WT value (K_d = 79.1 pM). The affinity of GDP (K_d = 22.3 pM) for this mutant has also increased by a factor of 3. The lower K_d of both guanine nucleotides for this mutant is mainly due to the increase in k_{on}. Taken together, our fast kinetics results suggest that the G60A mutation increases by a mechanism that is not well-understood, the affinity of the guanine nucleotides for Ras. This increase in affinity is lost because of the deletion of the long side chain of Lys147, which further exposes the guanine base to the solvent.

To examine how the double mutation affects catalyzed nucleotide release, we compared the rates of dissociation of nucleotide from WT-Ras and RasDM in the presence of the catalytic domain of Sos. Whereas equimolar concentrations of Sos (1 μM) substantially accelerate the release of GDP and GTP from WT-Ras (730×10^{-5} s^{-1}), they have a modest or no effect on both nucleotide-bound forms of RasDM [29×10^{-5} s^{-1} (Table 2)]. To rule out the possibility that a low binding affinity of RasDM for Sos is responsible for the low rate of nucleotide exchange, we performed a pull-down assay between Sos and the Ras proteins. Figure 3A shows that the catalytic domain of Sos binds to RasDM, albeit with a weaker affinity. Having shown binding, we repeated the exchange experiments in the presence of 10 μM Sos. Table 2 shows that despite the 10-fold excess, Sos is unable to accelerate dissociation of nucleotide from RasDM

Table 2: Rate and Equilibrium Constants for the Binding of GDP and GTP to Ras Proteins

	WT-Ras	RasG60A	RasDM
GDP			
K_1 (μM)	9.3	4.2	6.5
k_{+2} (s^{-1})	8.9	9.4	5.5
k_{on} ($\times 10^6$ M^{-1} s^{-1})	1.0	2.2	0.8
$k_{off} = k_{-2}$ ($\times 10^{-5}$ s^{-1})	6.5[a]	5.0[a]	27.0
K_d*[b] (pM/relative)	68.0/1.0	22.3/0.3	319.0/4.7
k_{-2} ($\times 10^{-5}$ s^{-1}, with 1 μM Sos)	730	18.0	29.1
k_{-2} ($\times 10^{-5}$ s^{-1}, with 10 μM Sos)	2100	33.0	65.1
GTP			
K_1 (μM)	8.2	3.8	6.5
k_{+2} (s^{-1})	8.4	10.3	6.3
k_{on} ($\times 10^6$ M^{-1} s^{-1})	1.0	2.7	1.0
k_{-2} ($\times 10^{-5}$ s^{-1})	8.1	9.8	29.0
K_d* (pM/relative)	79.1/1	36.1/0.5	299.0/3.8

[a]Values from ref *26*. [b]$K_d = k_{-2}/k_{ON}$.

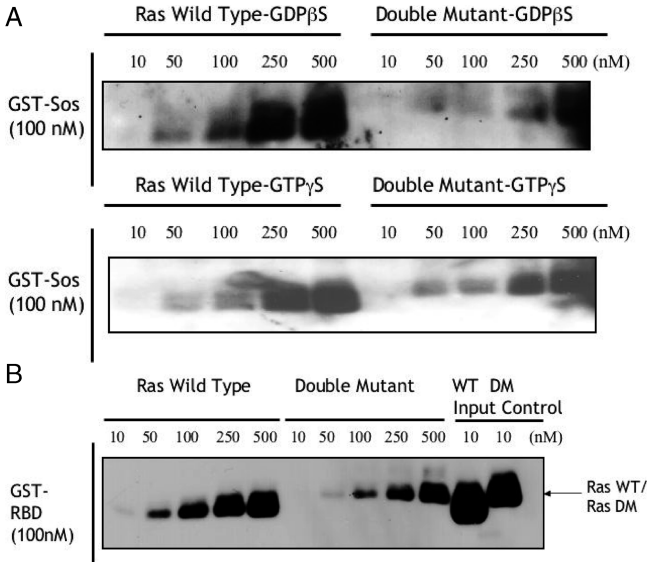

FIGURE 3: Binding of RasDM to the catalytic domain of Sos and to the Ras-binding domain (RBD) of Raf. (A) GST−Sos protein was incubated with increasing amounts of RasDM or wild-type untagged Ras loaded with GDPβS or GTPγS as indicated. Sos−Ras complexes were precipitated with GST beads, and the bound material was analyzed by Western blotting with anti-Ras antibodies. (B) GST−RafRBD protein (100 nM) was incubated with increasing amounts of wild-type or G60A/K147A untagged Ras proteins loaded with GTPγS as indicated. RafRBD−Ras complexes were precipitated with glutathione−Sepharose beads, and the bound material was analyzed by Western blotting with anti-Ras antibodies. Blotting for Ras shows that identical amounts were used in each pull-down experiment.

(65×10^{-5} s^{-1}) to the level of WT-Ras (2100×10^{-5} s^{-1}). The inability of Sos to accelerate exchange of nucleotide from RasDM is reminiscent of its inability to accelerate dissociation of nucleotide from RasG60A (*18*). It is unclear if the binding of Sos to RasDM stabilizes a RasDM·GXP−Sos ternary complex; however, it is very likely given that the ternary complex is stabilized in the case of RasG60A. Combined with the G60A data, our results demonstrate that flexibility at position 60 in Ras is required for Sos-catalyzed nucleotide exchange.

Binding to Raf and Activation of Erk in Cells. We have previously shown that when expressed in cells, approximately two-thirds of RasG60A is in the GTP-bound form (*18*). Because the structures of active RasG60A and RasDM are superposable and because the intrinsic rate of dissociation of nucleotide from RasDM is higher than that for RasG60A, it is likely that when expressed in cells at least a similar fraction of RasDM is also in the GTP-bound form. We therefore tested the ability of the open conformation of Ras to activate Erk.

Since to activate the MAP kinase pathway Ras has to bind to Raf, we first checked the ability of the open conformation of Ras to bind to RafRBD. Pull-down assays show that RasDM binds to RafRBD, albeit with a weaker affinity than WT-Ras (Figure 3B). To quantify the binding of RasDM to Raf, we used isothermal titration calorimetry (ITC) to measure the thermodynamics of binding of RafRBD to the GppNHp-bound form of RasG60A. We used the G60A mutant because of its stability. We do not expect major differences in the thermodynamics of the binding of G60A or the double mutant to RafRBD because of their structural and biochemical similarities. Before the ITC experiments, all proteins were dialyzed against the same DTT-free HEPES-containing buffer. Table 3 shows the primary results

Table 3: Thermodynamic Parameters of Association of RafRBD with Ras Proteins

	K_a ($\times 10^6$ M^{-1})	K_d (nM)	ΔH_0 (kcal/mol)	$T\Delta S_0$ (kcal/mol)
WT-Ras[a]	11.43 ± 0.86	88 ± 7	-2.46 ± 0.13	7.16 ± 0.09
RasG60A	1.16 ± 0.22	862 ± 189	-4.55 ± 0.76	3.71 ± 0.87
RasQ61G[a]	4.0 ± 1.25	250 ± 80	-4.36 ± 0.45	4.64 ± 0.63

[a]Values from ref *26*.

measured by the ITC experiments, K_a and ΔH_0, together with the calculated $T\Delta S_0$ and K_d ($= K_a^{-1}$) values. We measured a dissociation constant K_d of 862 nM for the RafRBD−RasG60A complex, a value ~10 times higher than that of the wild type (*26*, *29*). This decrease in affinity is due to a loss of 3.45 kcal/mol in the entropy of binding ($T\Delta S_0$ decreases from 7.16 to 3.71 kcal/mol) despite a more favorable enthalpy of binding (ΔH_0 decreases by 2.1 kcal/mol from −2.46 to −4.55 kcal/mol) (Table 3). The more favorable enthalpy of RafRBD binding of RasG60A compared to that of WT-Ras is rather surprising given the open conformation of the switch 1 region, the site of RafRBD binding. Interestingly, the measured enthalpy of binding (−4.55 kcal/mol) is within experimental error similar to the ΔH_0 (−4.36 kcal/mol) we reported under the same conditions for binding of RafRBD to the RasQ61G mutant in which switch 1 adopts a wild-type conformation favorable for effector binding. Thus, although the switch 1 regions of the G60A and Q61G mutants of Ras adopt opposing conformations in regard to effector binding, the ITC data show that the enthalpy of binding of RafRBD for both Ras mutants has barely changed. Combined, our ITC data support the conclusions that binding of RafRBD to Ras is entropy-driven and that the conformation of switch 2 is an important modulator of effector binding (*26*).

For the cell-based assays, cells were grown in the absence of serum and the dominant active RasG12V was used as a positive control. COS-1 cells were cotransfected with HA-tagged Erk and various amounts of T7-tagged Ras cDNA as indicated in Figure 4A. The cells were lysed, and the activation of Erk was analyzed by IP-Western blot using phospho-Erk specific antibodies. Figure 4A shows that as expected RasG12V efficiently activated Erk while only 2- and 3-fold increases in the level of Erk activation were observed for RasG60A and RasDM, respectively, even when cells were transfected with high cDNA concentrations (500 ng). These data demonstrate that the open conformation of Ras is unable to activate the MAP-kinase pathway, in accord with previous data showing that introducing the G60A mutation into v-H-Ras abolishes its transforming activity (*30*). The observed residual phosphorylation of Erk is consistent with the weak binding of the open conformation to RafRBD observed by ITC and pull-down assays.

Next, we tested the dominant negative properties of the open conformation of Ras and compared the abilities of RasG60A and RasDM to inhibit Erk activation in response to EGF stimulation in COS-1 cells. The dominant negative RasS17N was used as a positive control. COS-1 cells were cotransfected with the cDNAs of HA-tagged Erk, and the indicated T7-tagged Ras mutants. The cells were serum starved and stimulated with 100 ng/mL EGF for 10 min. Erk activation was assessed as described in the previous paragraph. As shown in Figure 4B, the G60A and G60A/K147A mutants of Ras inhibit Erk activation with RasDM slightly more efficiently than RasG60A. The level of inhibition is 70−80% of that of RasS17N, with RasDM slightly more efficient at inhibiting Erk phosphorylation than RasG60A,

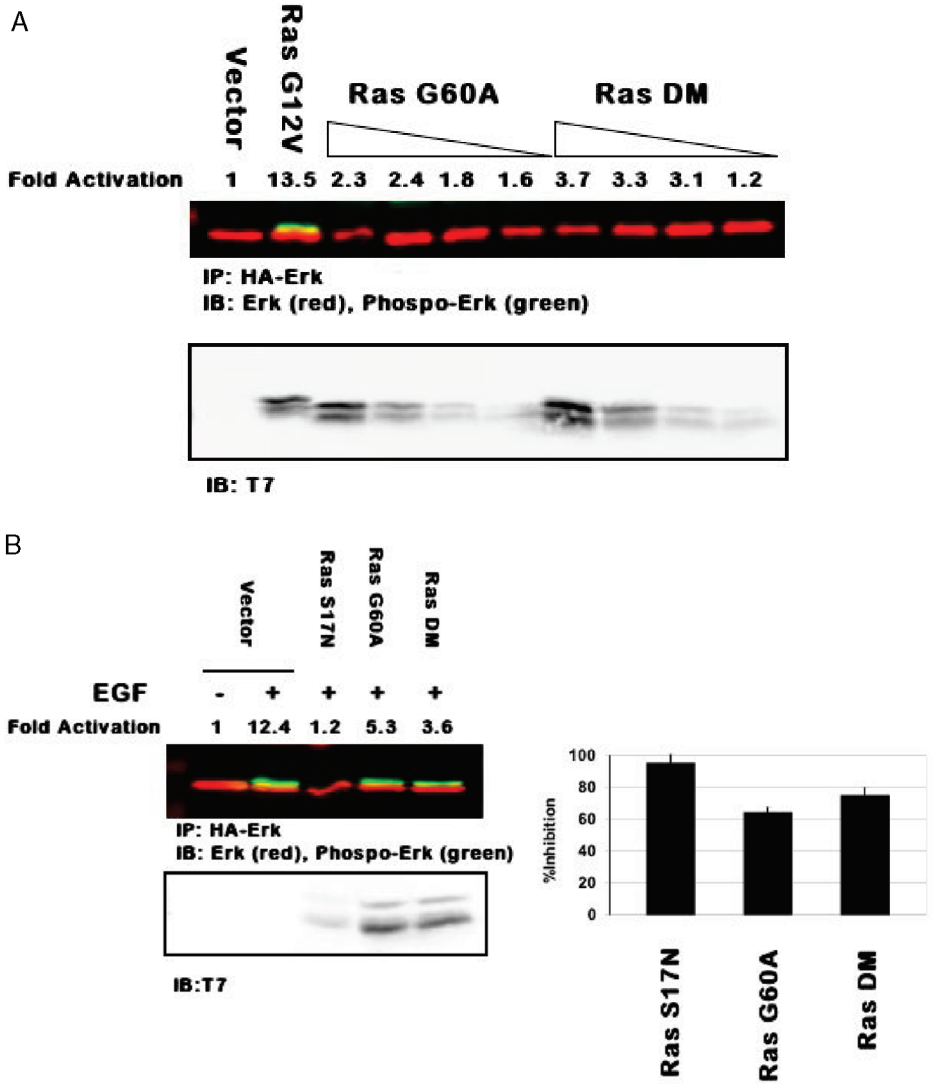

FIGURE 4: Cellular activity of RasDM. (A) COS-1 cells were transfected with HA-tagged Erk and the indicated T7-tagged Ras constructs (50, 100, 250, and 500 ng from right to left). The cells were allowed to express for 24 h prior to serum starvation for 8 h. The immune complexes were purified and incubated with either anti-T7 or anti-Erk2 and phospho-Erk1/2 antibodies and visualized. Relative Erk phosphorylation was quantified and normalized to total Erk expression. The dominant active RasG12V was used as a positive control. (B) Same as panel A, but cells stimulated with 100 ng/mL EGF. Lysates were subjected to Erk immunoprecipitation followed by immunoblotting with the indicated antibodies. As a control for EGF stimulation, the status of ERK phosphorylation was determined by transfecting cells with the dominant negative RasS17N.

suggesting that the open conformation behaves as a dominant negative protein in cells but not to the extent of RasS17N. One likely explanation for RasDM being a more effective dominant negative then RasG60A is that unlike RasG60A, both GDP- and GTP-bound structures of the double mutant adopt the open conformation, which is likely to better sequester Sos into a dead-end complex than the closed wild-type conformation adopted by RasG60A·GDP.

DISCUSSION

Here, we have characterized the first Ras mutant to adopt the same structure in the active and inactive forms. In both structures, the guanine nucleotide-binding site shows similarities to WT- and NF-Ras. For example, the guanine base makes conserved interactions with the ^{116}NKXD^{119} and ^{145}SAK^{147} motifs and the phosphates are stabilized by the P-loop as in WT-Ras while the conserved Phe28 and Thr35 are removed from stabilizing the guanine base and the Mg^{2+} ion as in NF-Ras. Two important remarks can be made here regarding the displacement of Phe28 from stabilizing the guanine base and the measured kinetics of nucleotide binding to RasDM. First, the constants (K_1 and k_{+2}) of GDP or GTP association are not affected by the double mutation, supporting the idea that mutations in the nucleotide-binding site of Ras affect the dissociation rather than association rate (*31*, *32*). Since the k_{+2} value is not affected by the G60A mutation alone or in combination with K147A, we conclude from the RasDM structure that the slow isomerization step observed by fluorescence spectroscopy could not be the closing of the switch regions on the nucleotide going from the open to the closed conformation. The molecular interpretation of this step is still unclear. Second, the 4-fold increase in the rate of nucleotide dissociation is relatively modest when compared to the 140-fold increase observed for GDP by the F28L mutation, which also changes the environment of the guanine base (*31*, *33*). From the open conformation of switch 1 in RasDM, one would predict that the rates of dissociation of nucleotide from RasDM should be at least equivalent to those measured for RasF28L. The structure of the RasF28L mutant is not available to explain at the molecular level the difference in the measured dissociation rates, but one likely explanation for this difference is the reduced

flexibility at position 60 in our Ras mutants but not in RasF28L. The reduced flexibility due to the G60A mutation prevents the conformational change necessary for dissociation of guanine nucleotide from Ras and therefore faster intrinsic and GEF-catalyzed nucleotide release. The absence of flexibility at the equivalent position (Gly226) in Gsα was also evoked to explain the inability of the Gsα(G226A) mutant to dissociate from the $\beta\gamma$ subunits when loaded with GTP (*34*, *35*).

We have also shown that in cells, the open conformation behaves as a dominant negative protein but not to the extent of RasS17N. The ability of the open conformation to sequester Sos when expressed in vivo is probably behind the dominant negative effect. The residual binding to Raf is the likely reason why RasG60A or RasDM does not inhibit Erk activation to the extent that RasS17N does. Our data thus confirm previous observations which showed that inhibiting the activation of endogenous Ras is not enough for a Ras mutant to acquire a dominant negative character but that it should also be unable to activate downstream effectors (*36*).

We find it remarkable that while the GDP-bound forms of the G60A and K147A single mutants adopt structures that resemble that of WT-Ras, mutating both residues, which are ~20 Å apart and interact with different parts of the nucleotide, results in a protein that adopts a structure that resembles NF-Ras as found in the complex with Sos. In the context of wild-type Ras, this observation suggests the existence of an exchange of structural information between the nucleotide binding motifs of Ras. We have previously reported such exchange between the switch regions during GTP hydrolysis and effector binding (*26*, *37*). How the structural information between the different nucleotide binding motifs is exchanged requires further investigation. Finally, although mutations affecting positions 60 and 147 are not common in human cancers (*38*), the G60R mutation in K-Ras has been found in patients diagnosed with the cardio-facio-cutaneous syndrome (*39*). Whether the G60R mutation, which should decrease the flexibility of the ^{57}DTAGQ^{61} sequence, stabilizes the open conformation of active Ras, prevents activation by Sos, and therefore is behind the observed phenotype in those patients remains to be seen.

Lastly, does the open conformation mimic the structure of an intermediate or transition state during Ras cycling? A likely answer to this question can be found in the nucleotide exchange cycle shown in Scheme 1 (*13*, *20*). Three observations can be made from this widely accepted scheme. First, this scheme is independent of the nature of the guanine nucleotide since within experimental error, there is no difference in the measured rate constants for GDP versus GTP binding to Ras. This observation suggests that binding of GDP and GTP to and release of GDP and GTP from NF-Ras follow the same reaction path so that the structures of the Ras·GDP$_L$ and Ras·GTP$_L$ loose complexes are to a first approximation identical. Second, it is also expected that the intrinsic rates of dissociation of nucleotide from Ras·GXP$_L$ is faster than those of Ras·GXP$_T$ (i.e., WT-Ras) since the nucleotide for this intermediate is loosely bound. Third, given that it is an intermediate going from NF- to WT-Ras, the structure of Ras·GXP$_L$ should bear resemblance to both structures. Our crystallographic and fluorescence data show that RasDM fits all three characteristics. Whether RasDM mimics the structure of the intermediate for nucleotide exchange Ras·GXP$_L$ remains to be seen.

ACKNOWLEDGMENT

We thank Annie Héroux for technical assistance at beamline X26C.

REFERENCES

1. Downward, J. (2003) Targeting RAS signalling pathways in cancer therapy. *Nat. Rev. Cancer 3*, 11–22.
2. Vojtek, A. B., and Der, C. J. (1998) Increasing complexity of the Ras signaling pathway. *J. Biol. Chem. 273*, 19925–19928.
3. Bourne, H. R., Sanders, D. A., and McCormick, F. (1990) The GTPase superfamily: A conserved switch for diverse cell functions. *Nature 348*, 125–132.
4. Chardin, P., Camonis, J. H., Gale, N. W., van Aelst, L., Schlessinger, J., Wigler, M. H., and Bar-Sagi, D. (1993) Human Sos1: A guanine nucleotide exchange factor for Ras that binds to GRB2. *Science 260*, 1338–1343.
5. Sprang, S. R., and Coleman, D. E. (1998) Invasion of the nucleotide snatchers: Structural insights into the mechanism of G protein GEFs. *Cell 95*, 155–158.
6. Cherfils, J., and Chardin, P. (1999) GEFs: Structural basis for their activation of small GTP-binding proteins. *Trends Biochem. Sci. 24*, 306–311.
7. Chau, V., Romero, G., and Biltonen, R. L. (1981) Kinetic studies on the interactions of *Escherichia coli* K12 elongation factor Tu with GDP and elongation factor Ts. *J. Biol. Chem. 256*, 5591–5596.
8. Hwang, Y. W., and Miller, D. L. (1985) A study of the kinetic mechanism of elongation factor Ts. *J. Biol. Chem. 260*, 11498–11502.
9. Romero, G., Chau, V., and Biltonen, R. L. (1985) Kinetics and thermodynamics of the interaction of elongation factor Tu with elongation factor Ts, guanine nucleotides, and aminoacyl-tRNA. *J. Biol. Chem. 260*, 6167–6174.
10. Bourne, H. R., Sanders, D. A., and McCormick, F. (1991) The GTPase superfamily: Conserved structure and molecular mechanism. *Nature 349*, 117–127.
11. Stryer, L. (1985) Molecular design of an amplification cascade in vision. *Biopolymers 24*, 29–47.
12. Klebe, C., Prinz, H., Wittinghofer, A., and Goody, R. S. (1995) The kinetic mechanism of Ran−nucleotide exchange catalyzed by RCC1. *Biochemistry 34*, 12543–12552.
13. Lenzen, C., Cool, R. H., Prinz, H., Kuhlmann, J., and Wittinghofer, A. (1998) Kinetic analysis by fluorescence of the interaction between Ras and the catalytic domain of the guanine nucleotide exchange factor Cdc25Mm. *Biochemistry 37*, 7420–7430.
14. Margarit, S. M., Sondermann, H., Hall, B. E., Nagar, B., Hoelz, A., Pirruccello, M., Bar-Sagi, D., and Kuriyan, J. (2003) Structural evidence for feedback activation by Ras·GTP of the Ras-specific nucleotide exchange factor SOS. *Cell 112*, 685–695.
15. Milburn, M. V., Tong, L., deVos, A. M., Brunger, A., Yamaizumi, Z., Nishimura, S., and Kim, S. H. (1990) Molecular switch for signal transduction: Structural differences between active and inactive forms of protooncogenic ras proteins. *Science 247*, 939–945.
16. Pai, E. F., Kabsch, W., Krengel, U., Holmes, K. C., John, J., and Wittinghofer, A. (1989) Structure of the guanine-nucleotide-binding domain of the Ha-ras oncogene product p21 in the triphosphate conformation. *Nature 341*, 209–214.
17. Boriack-Sjodin, P. A., Margarit, S. M., Bar-Sagi, D., and Kuriyan, J. (1998) The structural basis of the activation of Ras by Sos. *Nature 394*, 337–343.
18. Ford, B., Skowronek, K., Boykevisch, S., Bar-Sagi, D., and Nassar, N. (2005) Structure of the G60A mutant of Ras: Implications for the dominant negative effect. *J. Biol. Chem. 280*, 25697–25705.
19. Hall, B. E., Yang, S. S., Boriack-Sjodin, P. A., Kuriyan, J., and Bar-Sagi, D. (2001) Structure-based mutagenesis reveals distinct functions for Ras switch 1 and switch 2 in Sos-catalyzed guanine nucleotide exchange. *J. Biol. Chem. 276*, 27629–27637.
20. John, J., Sohmen, R., Feuerstein, J., Linke, R., Wittinghofer, A., and Goody, R. S. (1990) Kinetics of interaction of nucleotides with nucleotide-free H-ras p21. *Biochemistry 29*, 6058–6065.
21. Otwinowski, Z., Borek, D., Majewski, W., and Minor, W. (2003) Multiparametric scaling of diffraction intensities. *Acta Crystallogr. A59*, 228–234.
22. Navaza, J., and Saludjian, P. (1997) AMoRe: An automated Molecular Replacement Program Package. *Methods Enzymol. 276*, 581–594.
23. Winn, M. D., Isupov, M. N., and Murshudov, G. N. (2001) Use of TLS parameters to model anisotropic displacements in macromolecular refinement. *Acta Crystallogr. D57*, 122–133.
24. Murshudov, G. N., Vagin, A. A., and Dodson, E. J. (1997) Refinement of macromolecular structures by the maximum-likelihood method. *Acta Crystallogr. D53*, 240–255.
25. Laskowski, R. A., Moss, D. S., and Thornton, J. M. (1993) Main-chain bond lengths and bond angles in protein structures. *J. Mol. Biol. 231*, 1049–1067.

26. Ford, B., Hornak, V., Kleinman, H., and Nassar, N. (2006) Structure of a transient intermediate for GTP hydrolysis by ras. *Structure 14*, 427–436.
27. Bradford, M. M. (1976) A rapid and sensitive method for the quantitation of microgram quantities of protein utilizing the principle of protein-dye binding. *Anal. Biochem. 72*, 248–254.
28. Hubbard, S. J., and Thornton, J. M. (1993) NACCESS , University College, London.
29. Rudolph, M. G., Linnemann, T., Grunewald, P., Wittinghofer, A., Vetter, I. R., and Herrmann, C. (2001) Thermodynamics of Ras/effector and Cdc42/effector interactions probed by isothermal titration calorimetry. *J. Biol. Chem. 276*, 23914–23921.
30. Sung, Y. J., Carter, M., Zhong, J. M., and Hwang, Y. W. (1995) Mutagenesis of the H-ras p21 at glycine-60 residue disrupts GTP-induced conformational change. *Biochemistry 34*, 3470–3477.
31. Reinstein, J., Schlichting, I., Frech, M., Goody, R. S., and Wittinghofer, A. (1991) p21 with a phenylalanine 28 → leucine mutation reacts normally with the GTPase activating protein GAP but nevertheless has transforming properties. *J. Biol. Chem. 266*, 17700–17706.
32. Schmidt, G., Lenzen, C., Simon, I., Deuter, R., Cool, R. H., Goody, R. S., and Wittinghofer, A. (1996) Biochemical and biological consequences of changing the specificity of p21ras from guanosine to xanthosine nucleotides. *Oncogene 12*, 87–96.
33. Schlichting, I., John, J., Frech, M., Chardin, P., Wittinghofer, A., Zimmermann, H., and Rosch, P. (1990) Proton NMR studies of transforming and nontransforming H-ras p21 mutants. *Biochemistry 29*, 504–511.
34. Miller, R. T., Masters, S. B., Sullivan, K. A., Beiderman, B., and Bourne, H. R. (1988) A mutation that prevents GTP-dependent activation of the α chain of Gs. *Nature 334*, 712–715.
35. Lee, E., Taussig, R., and Gilman, A. G. (1992) The G226A mutant of Gsα highlights the requirement for dissociation of G protein subunits. *J. Biol. Chem. 267*, 1212–1218.
36. Cool, R. H., Schmidt, G., Lenzen, C. U., Prinz, H., Vogt, D., and Wittinghofer, A. (1999) The Ras mutant D119N is both dominant negative and activated. *Mol. Cell. Biol. 19*, 6297–6305.
37. Hall, B. E., Bar-Sagi, D., and Nassar, N. (2002) The structural basis for the transition from Ras-GTP to Ras-GDP. *Proc. Natl. Acad. Sci. U.S.A. 99*, 12138–12142.
38. Bos, J. L. (1989) ras oncogenes in human cancer: A review. *Cancer Res. 49*, 4682–4689.
39. Niihori, T., Aoki, Y., Narumi, Y., Neri, G., Cave, H., Verloes, A., Okamoto, N., Hennekam, R. C., Gillessen-Kaesbach, G., Wieczorek, D., Kavamura, M. I., Kurosawa, K., Ohashi, H., Wilson, L., Heron, D., Bonneau, D., Corona, G., Kaname, T., Naritomi, K., Baumann, C., Matsumoto, N., Kato, K., Kure, S., and Matsubara, Y. (2006) Germline KRAS and BRAF mutations in cardio-facio-cutaneous syndrome. *Nat. Genet. 38*, 294–296.
40. Kraulis, P. J. (1991) MOLSCRIPT: A program to produce both detailed and schematic plots of protein structures. *J. Appl. Crystallogr. 24*, 946–950.
41. Brünger, A. T. (1992) Free R value: A novel statistical quantity for assessing the accuracy of crystal structures. *Nature 355*, 472–475.